The multi-vicinal fluoroalkane motif: An examination of 2,3,4,5-tetrafluorohexane stereoisomers

Luke Hunter,* Peer Kirsch,[†] John T. G. Hamilton[‡] and David O'Hagan*

SUPPORTING INFORMATION

* *Centre for Biomolecular Sciences and School of Chemistry*
University of St Andrews, Fife KY169ST, United Kingdom

[†] *Merck Ltd. Japan, Liquid Crystal Technical Center*
4084 Nakatsu, Aikawa-machi, Aiko-gun, 243-0303 Kanagawa, Japan

[‡] *Food Chemistry Branch*
Agri-Food Biosciences Institute, Belfast BT9 5PX, United Kingdom

Contents:

NMR analyses…….. S-2
GC-MS spectra……..... S-28
Computational details…….. S-31

Figure S1. ^{1}H NMR spectrum (400 MHz, 80:20 v/v $CDCl_3/D_8$-THF) of **1a**

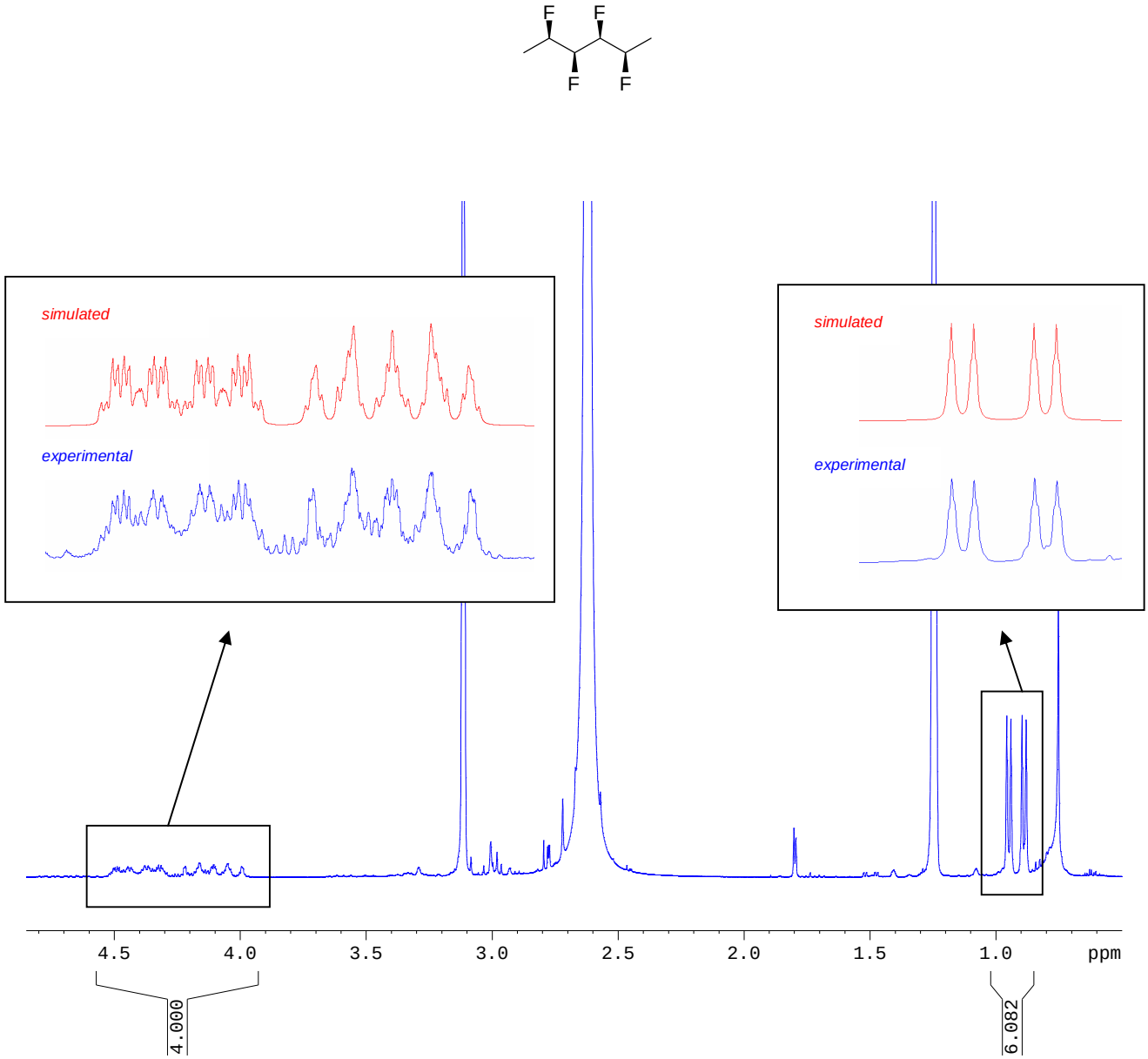

Figure S2: $^{1}H,^{1}H$ 2D-COSY (300 MHz, 80:20 v/v $CDCl_3/D_8$-THF) of **1a**

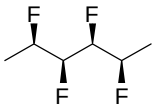

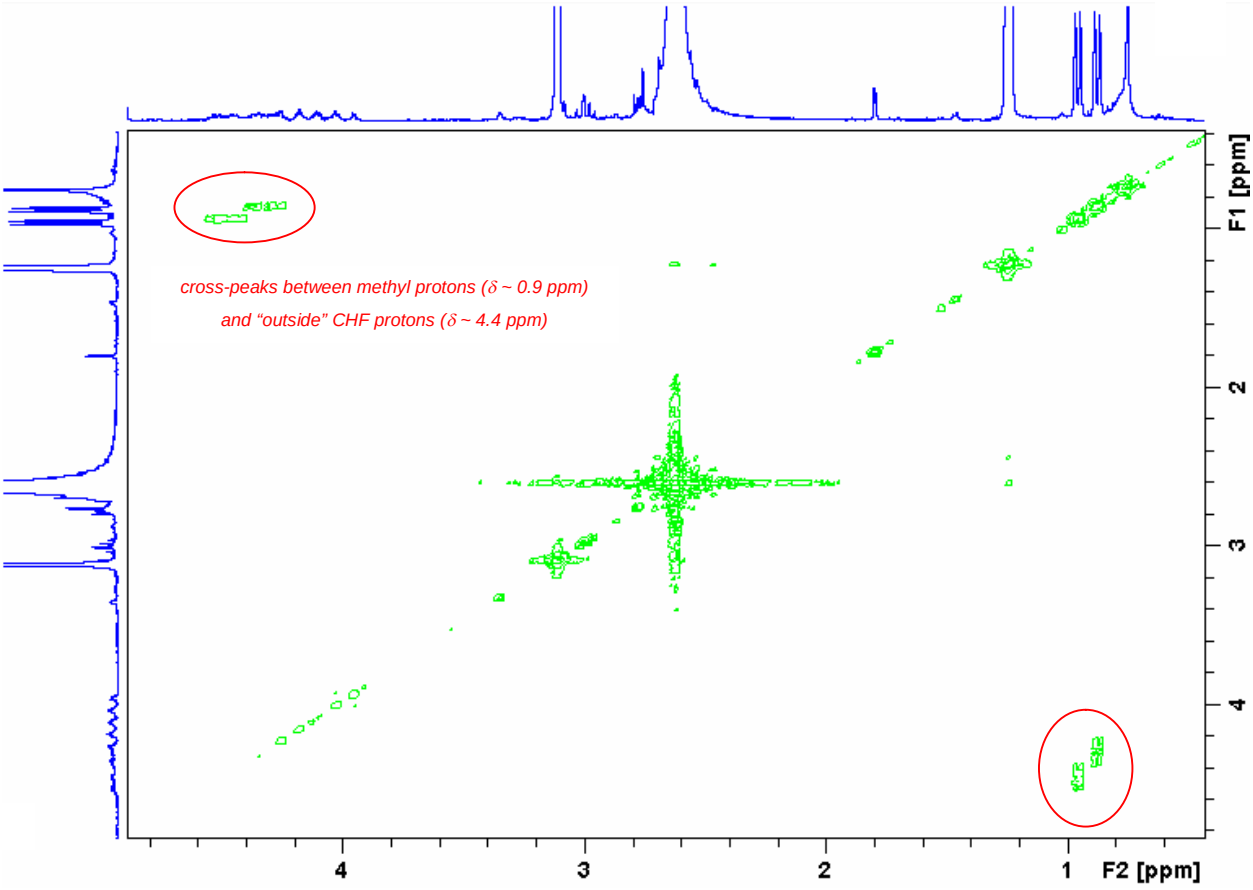

Figure S3. ^{19}F NMR (376 MHz, 80:20 v/v $CDCl_3/D_8$-THF) of **1a**

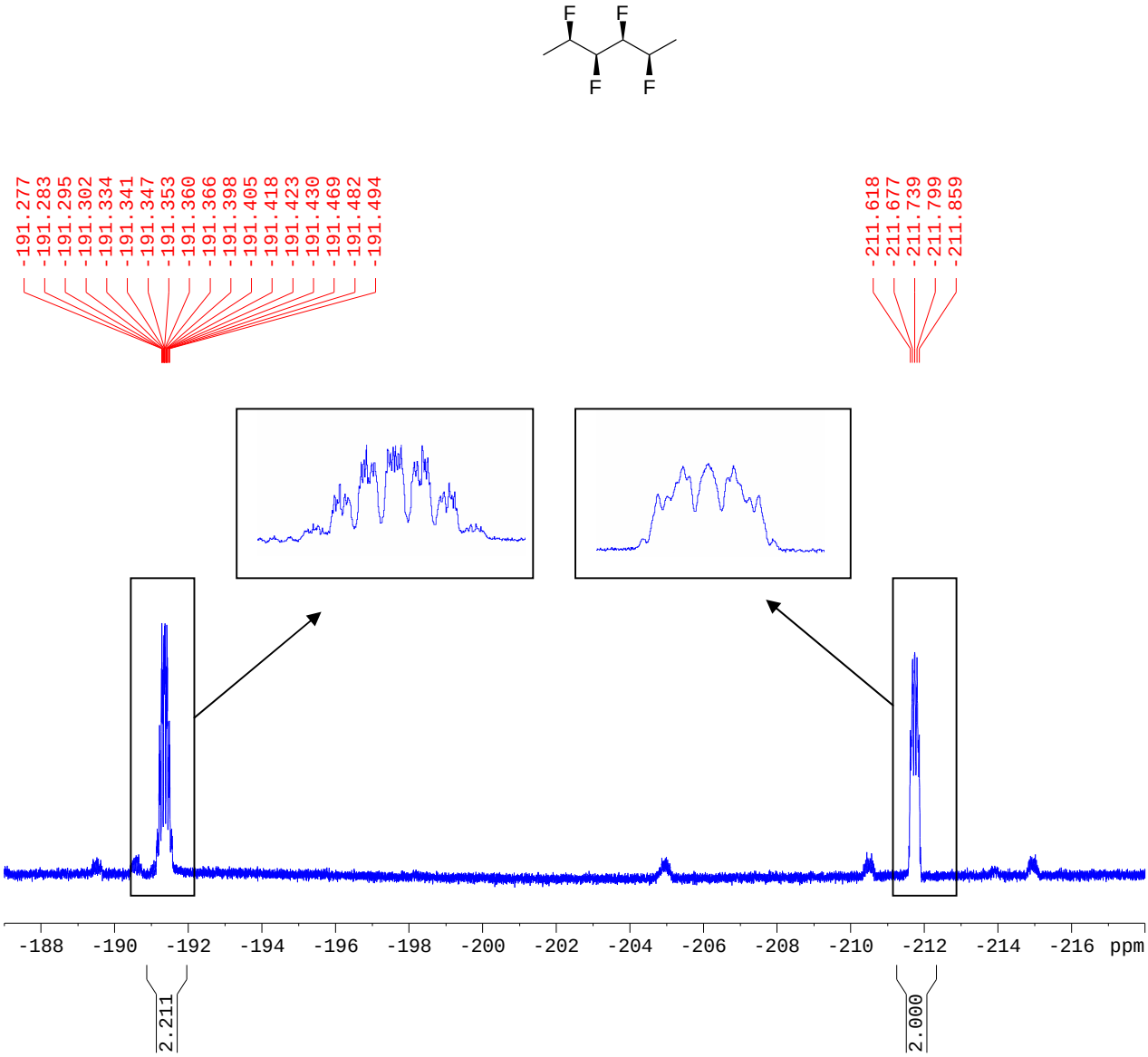

Figure S4. ^{19}F {^{1}H dec} NMR (376 MHz, 80:20 v/v $CDCl_3/D_8$-THF) of **1a**

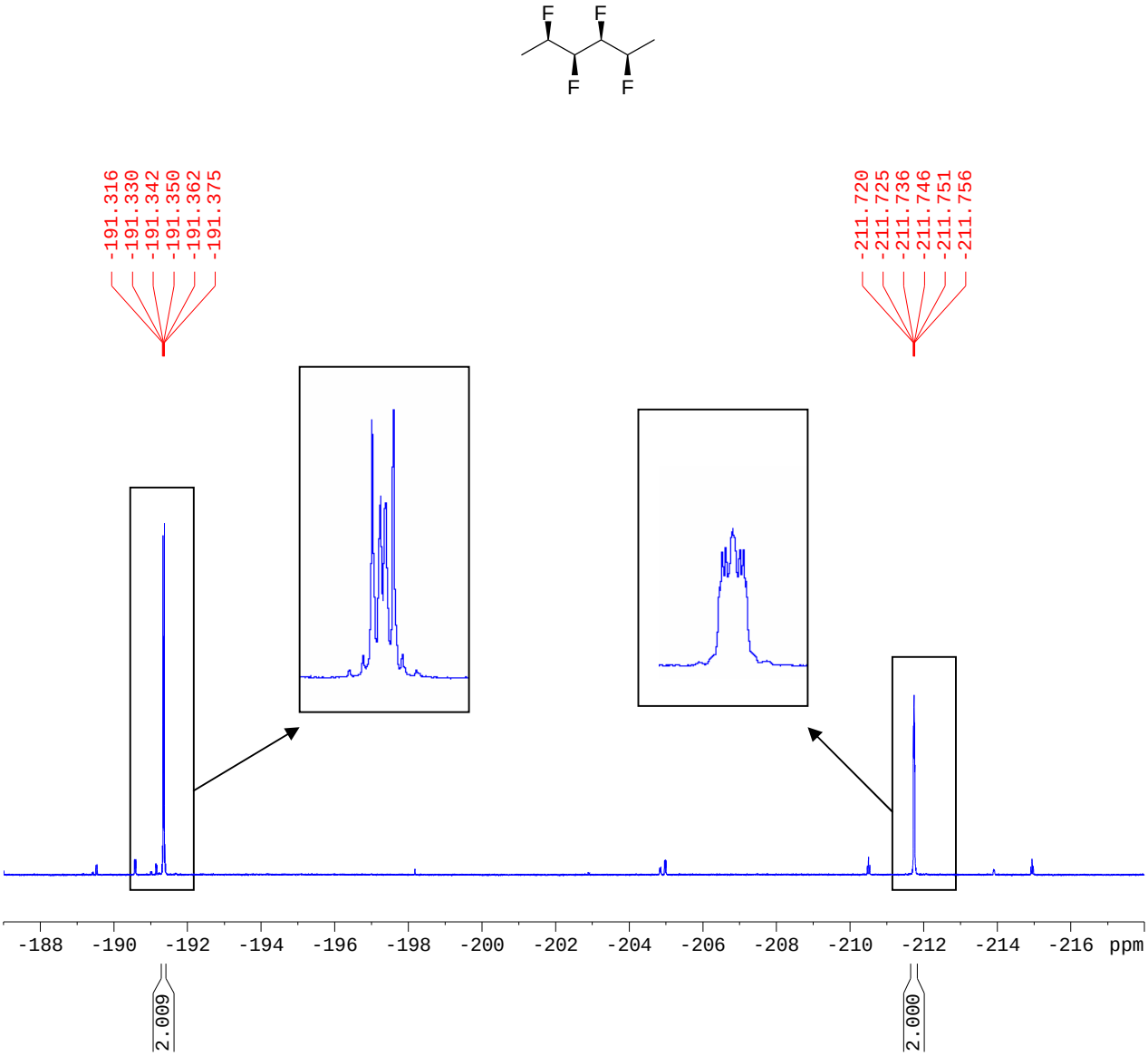

Figure S5. 2D $^{1}H,^{13}C$ HSQC with adiabatic pulses (500 MHz, 80:20 v/v $CDCl_3/D_8$-THF) of **1a**

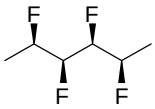

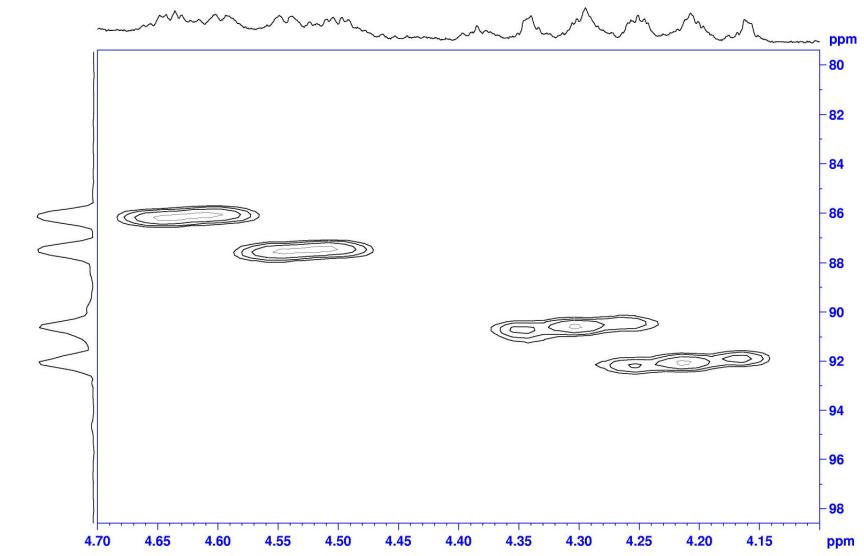

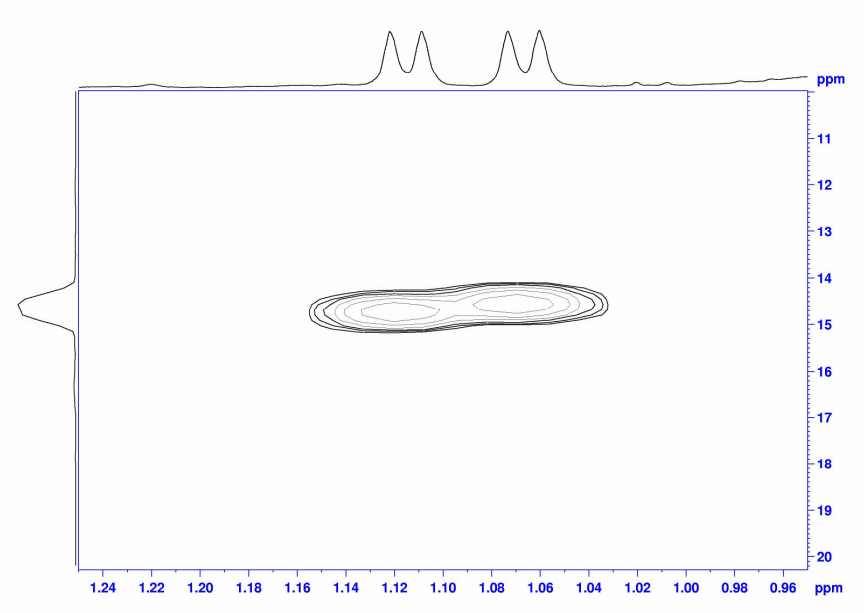

Table S1.[a] Calculated coupling constants for **1a**

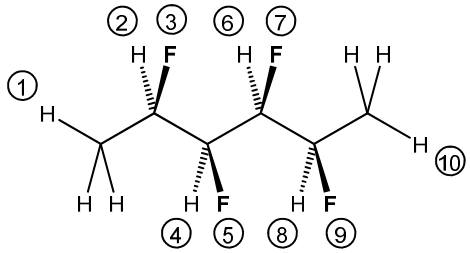

	2	**3**	**4**	**5**	**6**	**7**	**8**	**9**	**10**
1	6.5	24.1	0.0	0.9	0.0	0.9	0.0	0.0	0.0
2		47.7	3.2	21.5	0.0	1.0	0.0	0.0	0.0
3			22.4	N/D	0.0	N/D	0.0	N/D	0.0
4				48.2	6.19	18.1	0.0	0.0	0.0
5					18.1	N/D	1.0	N/D	0.9
6						48.2	3.2	22.4	0.0
7							21.5	N/D	0.9
8								47.7	6.5
9									24.1

[a] The $^{3}J_{HH}$ and $^{3}J_{HF}$ values were obtained from the simulated ^{1}H NMR spectrum (Figure S1). The $^{3}J_{FF}$ values were not determined (N/D) because the ^{19}F NMR and ^{19}F {^{1}H dec} NMR spectra (Figures S3 and S4) were not amenable to simulation due to poor peak shape and resolution.

Figure S6. Variable-temperature ^{1}H NMR (500 MHz, 80:20 v/v $CDCl_3/D_8$-THF) of **1a**

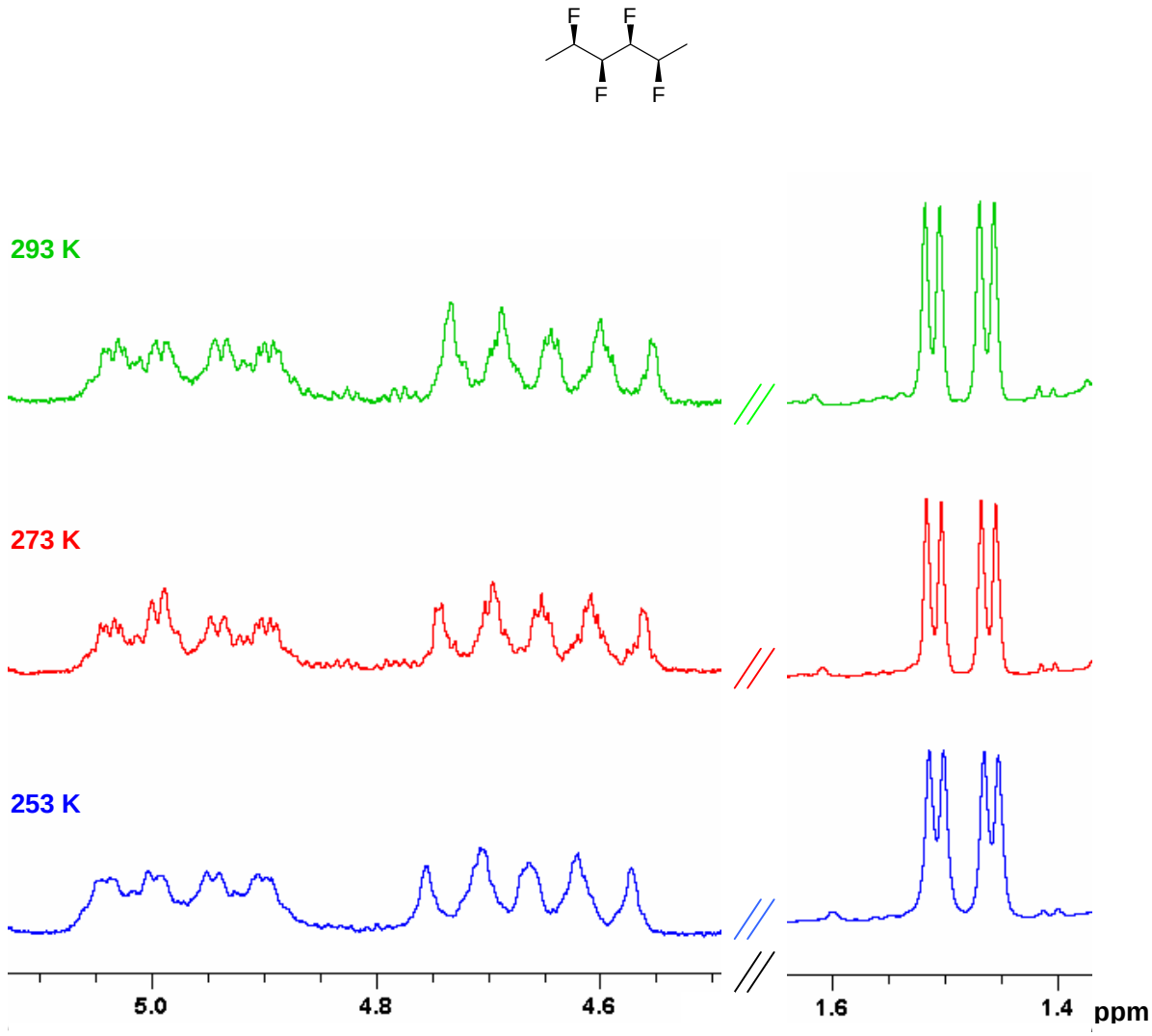

Figure S7. Variable-temperature ^{19}F NMR (470 MHz, 80:20 v/v $CDCl_3/D_8$-THF) of **1a**

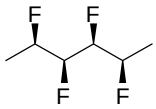

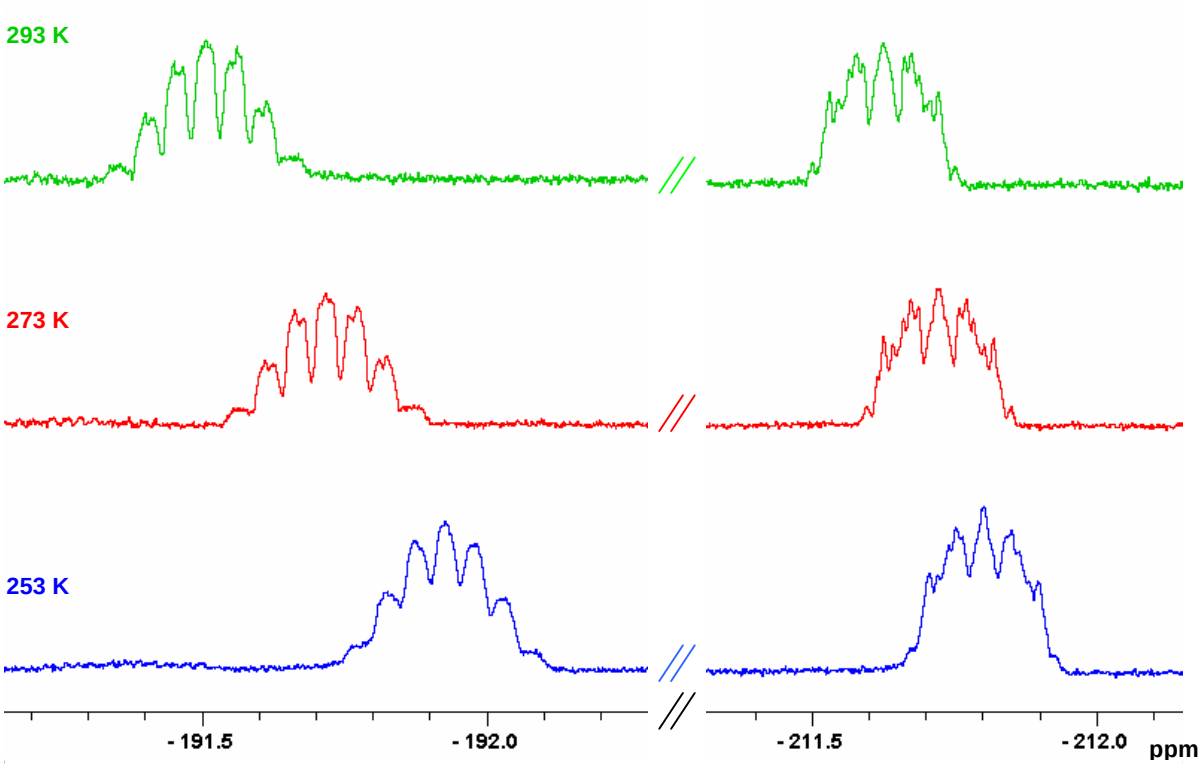

Figure S8. Variable-temperature ^{19}F {^{1}H dec} NMR (470 MHz, 80:20 v/v $CDCl_3/D_8$-THF) of **1a**

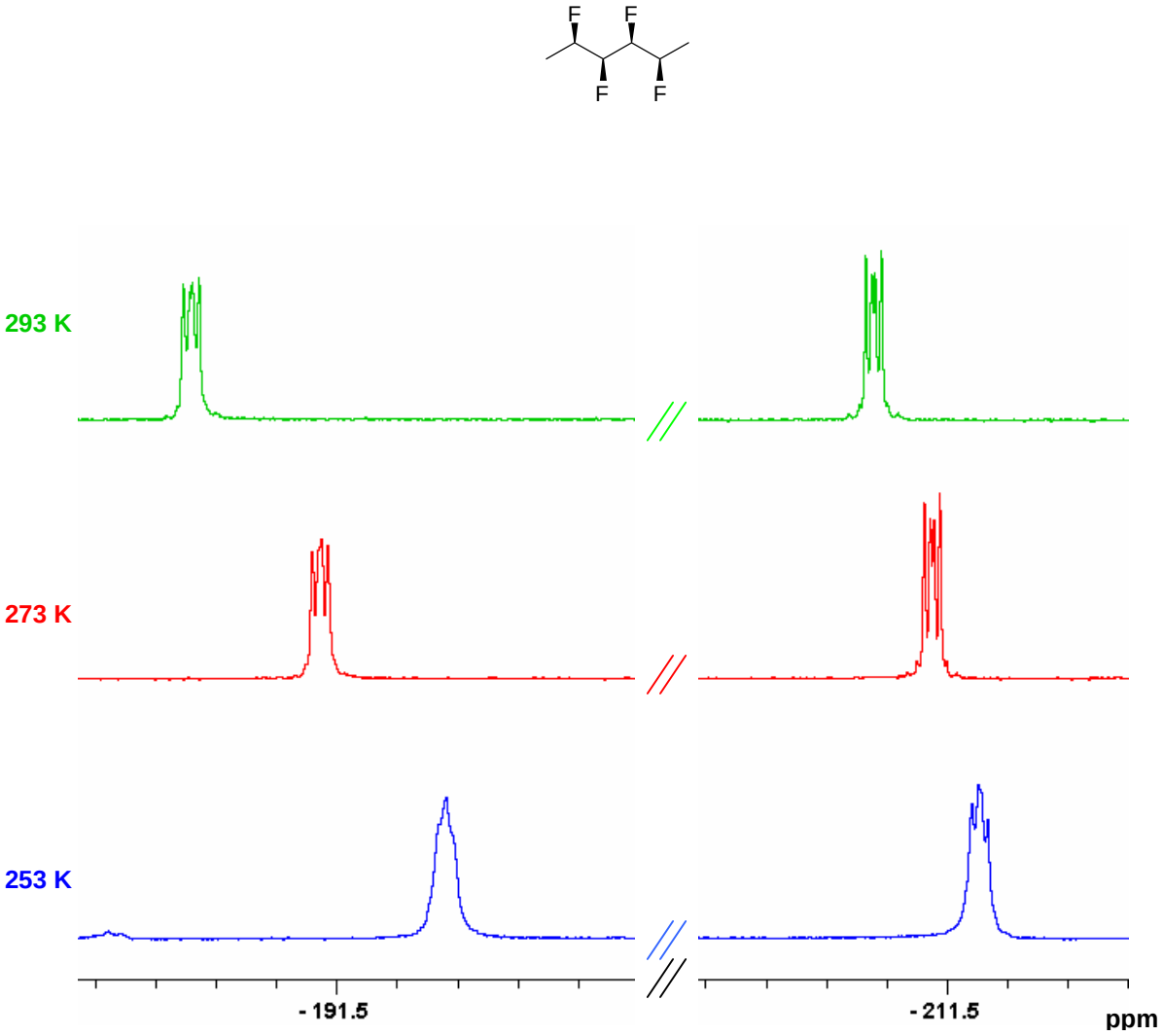

Figure S9.[a] ^{1}H NMR (400 MHz, 76:24 v/v $CDCl_3$/THF) of **1b**

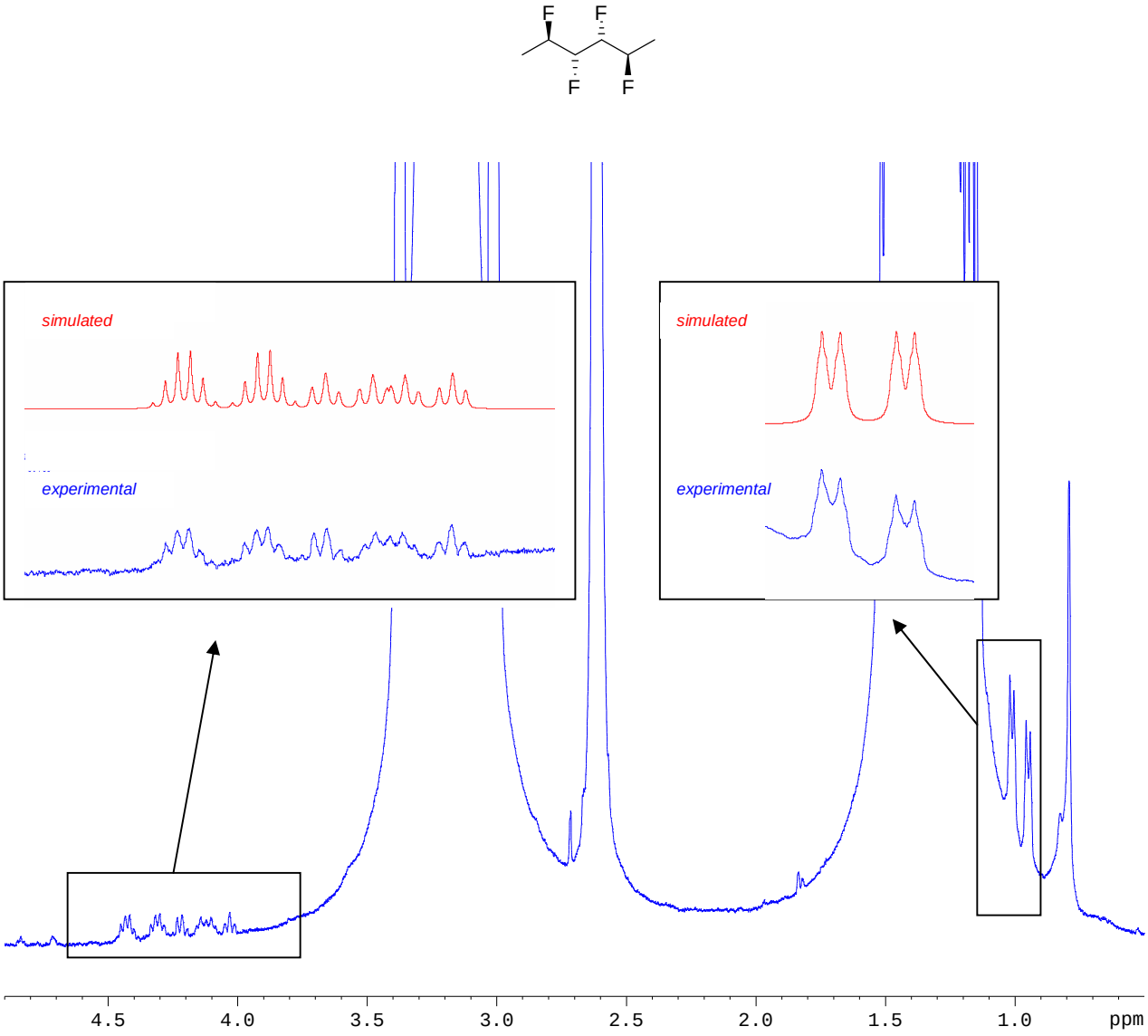

[a] This spectrum was obtained after performing the reaction in tetrahydrofuran rather than D_8-tetrahydrofuran, hence the large solvent peaks. A subsequent repetition of the reaction using D_8-tetrahydrofuran as the solvent provided the ^{19}F NMR spectra below (Figures S10 and S11), but the ^{1}H NMR spectrum from the reaction in D_8-tetrahydrofuran contained a masking impurity in the fluoroalkyl region.

Figure S10. ^{19}F NMR (376 MHz, 76:24 v/v $CDCl_3/D_8$-THF) of **1b**

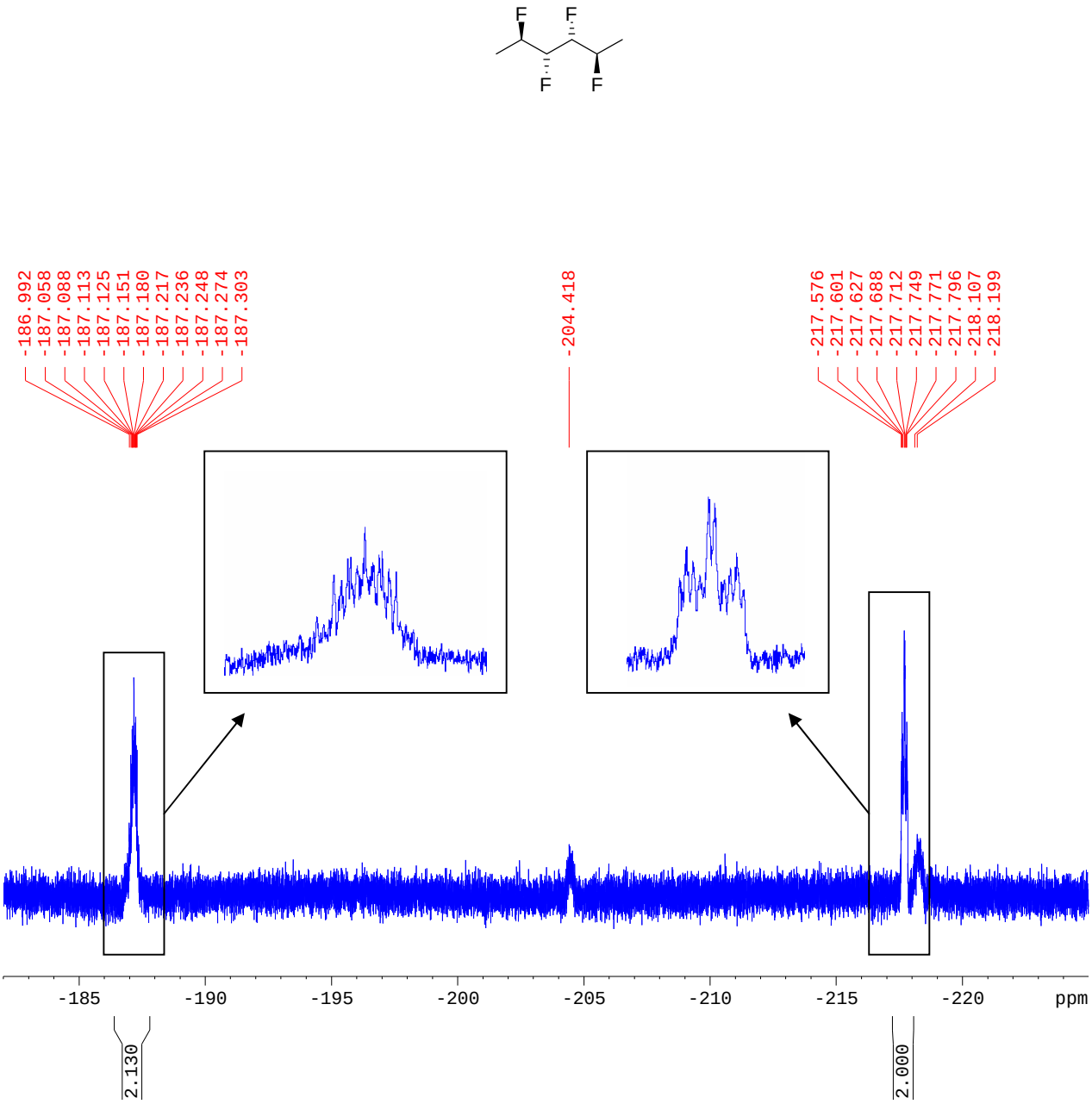

Figure S11. ^{19}F {^{1}H dec} NMR (376 MHz, 76:24 v/v $CDCl_3/D_8$-THF) OF **1b**

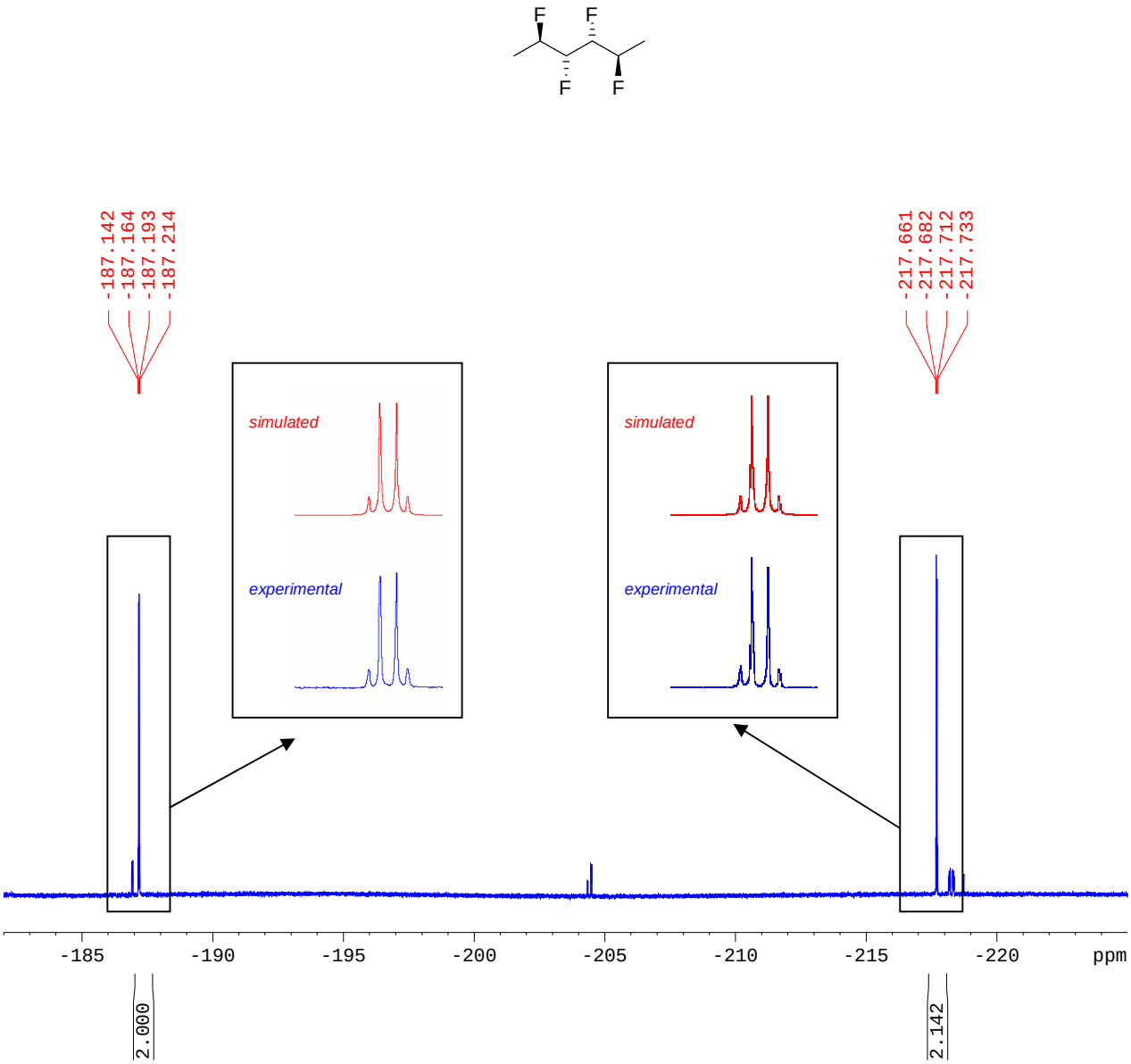

Figure S12. 2D $^{1}H,^{13}C$ HSQC with adiabatic pulses (500 MHz, 76:24 v/v $CDCl_3/D_8$-THF) of **1b**

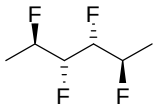

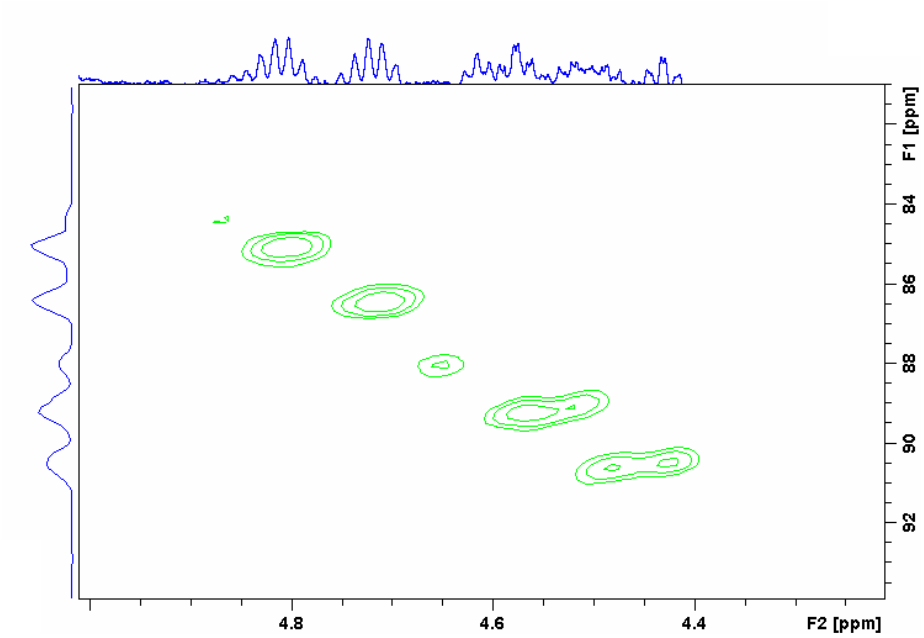

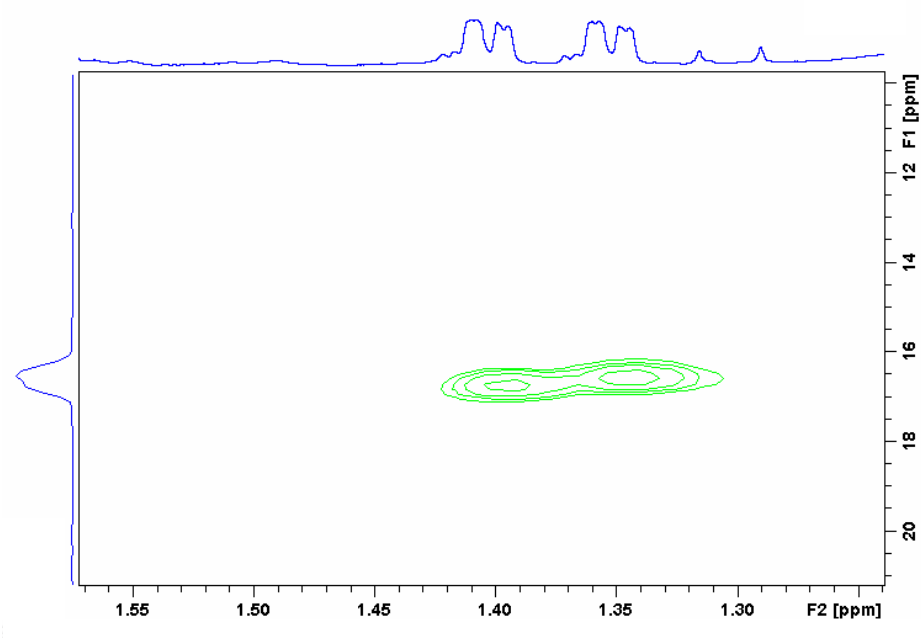

Table S2.[a] Calculated coupling constants for **1b**

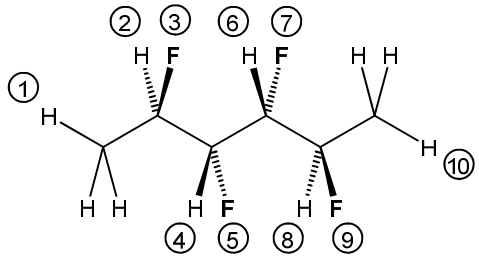

	2	**3**	**4**	**5**	**6**	**7**	**8**	**9**	**10**
1	6.2	25.2	0.0	1.5	0.0	1.5	0.0	0.0	0.0
2		47.0	7.2	7.2	0.0	0.0	0.0	0.0	0.0
3			8.5	14.4	0.0	2.7	0.0	0.4	0.0
4				47.0	1.3	28.0	0.0	0.0	0.0
5					28.0	8.2	0.0	2.7	1.5
6						47.0	7.2	8.5	0.0
7							7.2	14.4	1.5
8								47.0	6.2
9									25.2

[a] The $^{3}J_{HH}$ and $^{3}J_{HF}$ values were obtained from the simulated ^{1}H NMR spectrum (Figure S9). The $^{3}J_{FF}$ values were obtained from the simulated ^{19}F {^{1}H dec} NMR spectrum (Figure S11).

Figure S13. Variable-temperature ^{1}H NMR (500 MHz, 76:24 v/v $CDCl_3/D_8$-THF) of **1b**

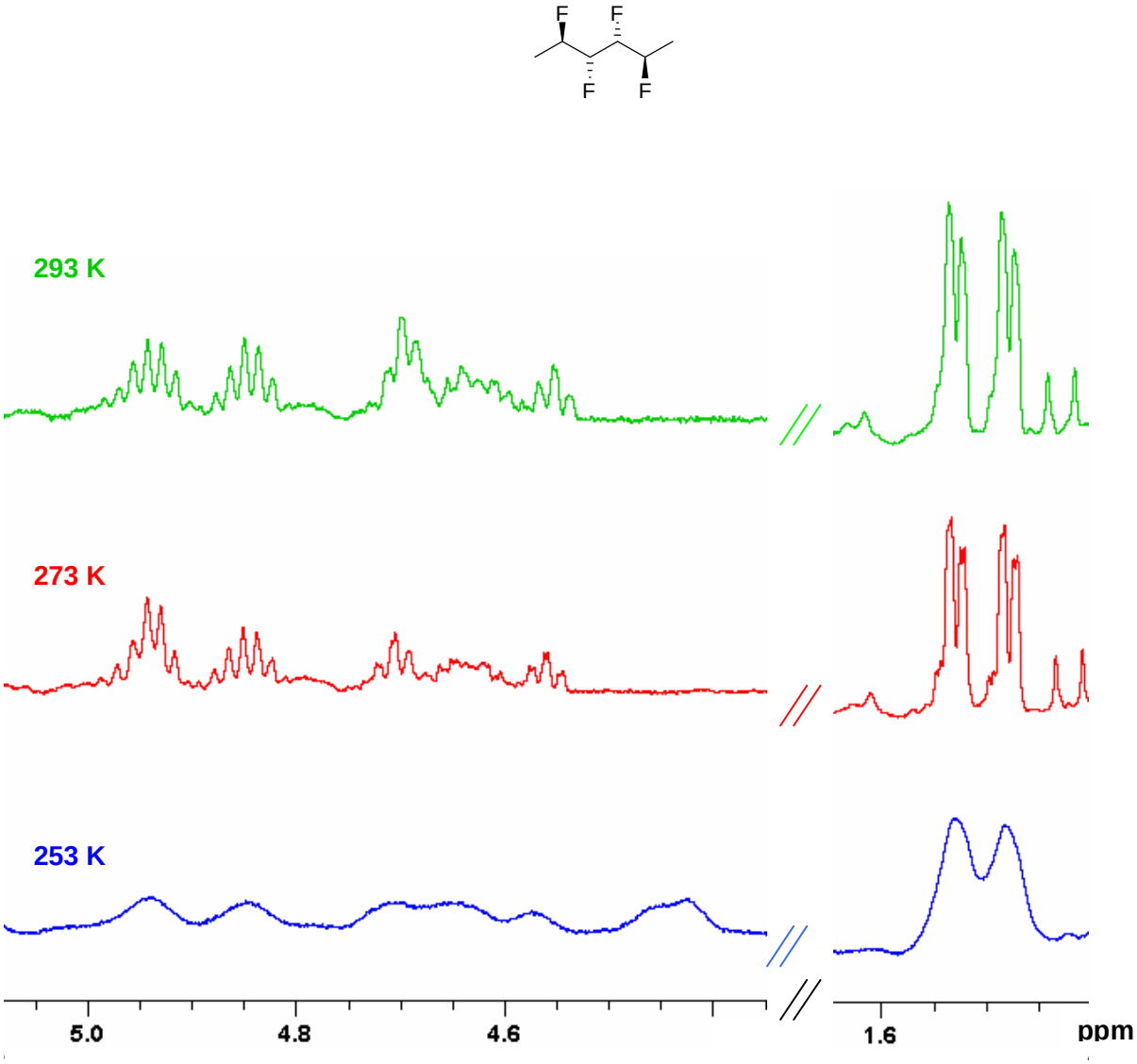

Figure S14. Variable-temperature ^{19}F NMR (470 MHz, 76:24 v/v $CDCl_3/D_8$-THF) of **1b**

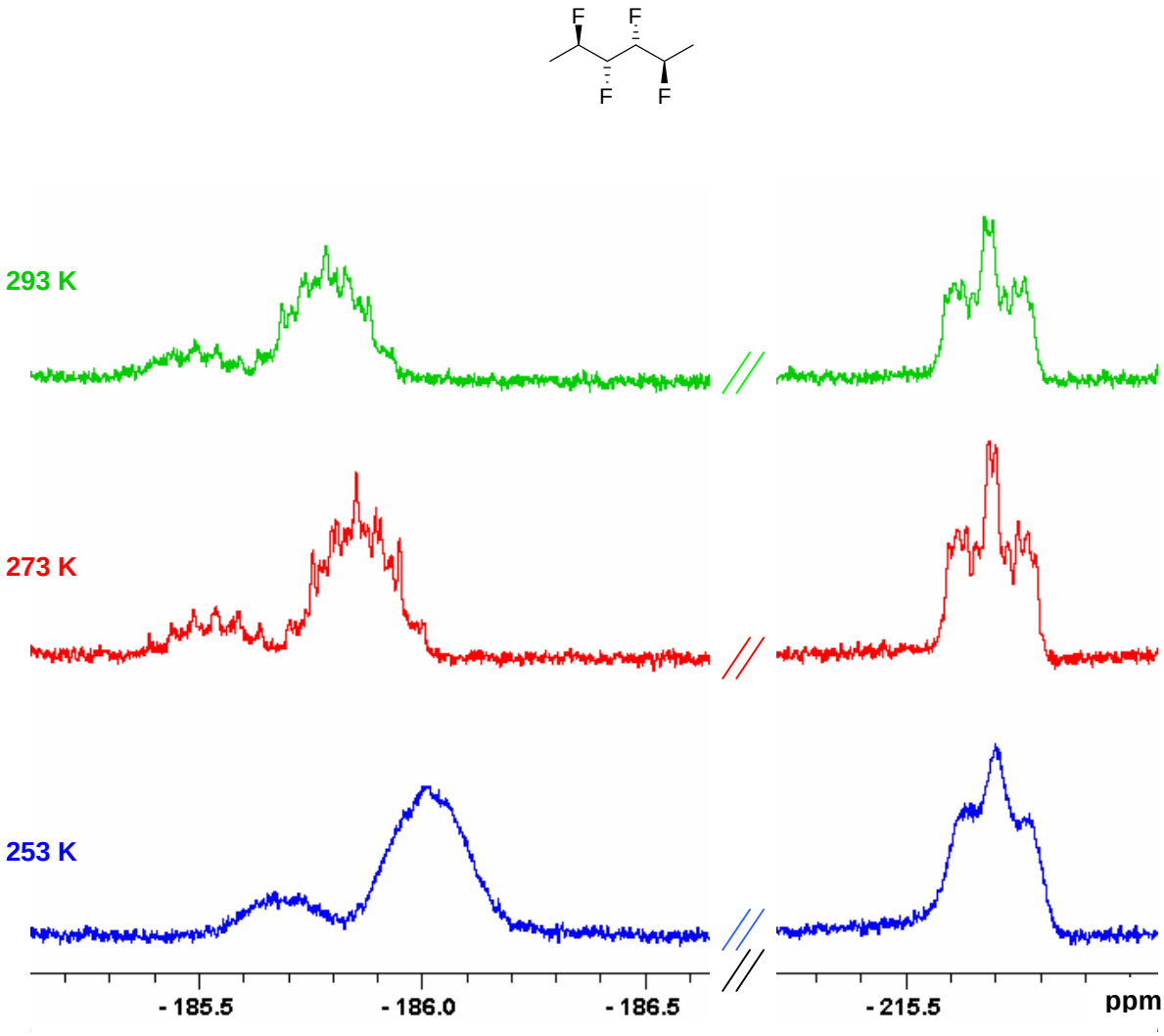

Figure S15. Variable-temperature ^{19}F {^{1}H dec} NMR (470 MHz, 76:24 v/v $CDCl_3/D_8$-THF) of **1b**

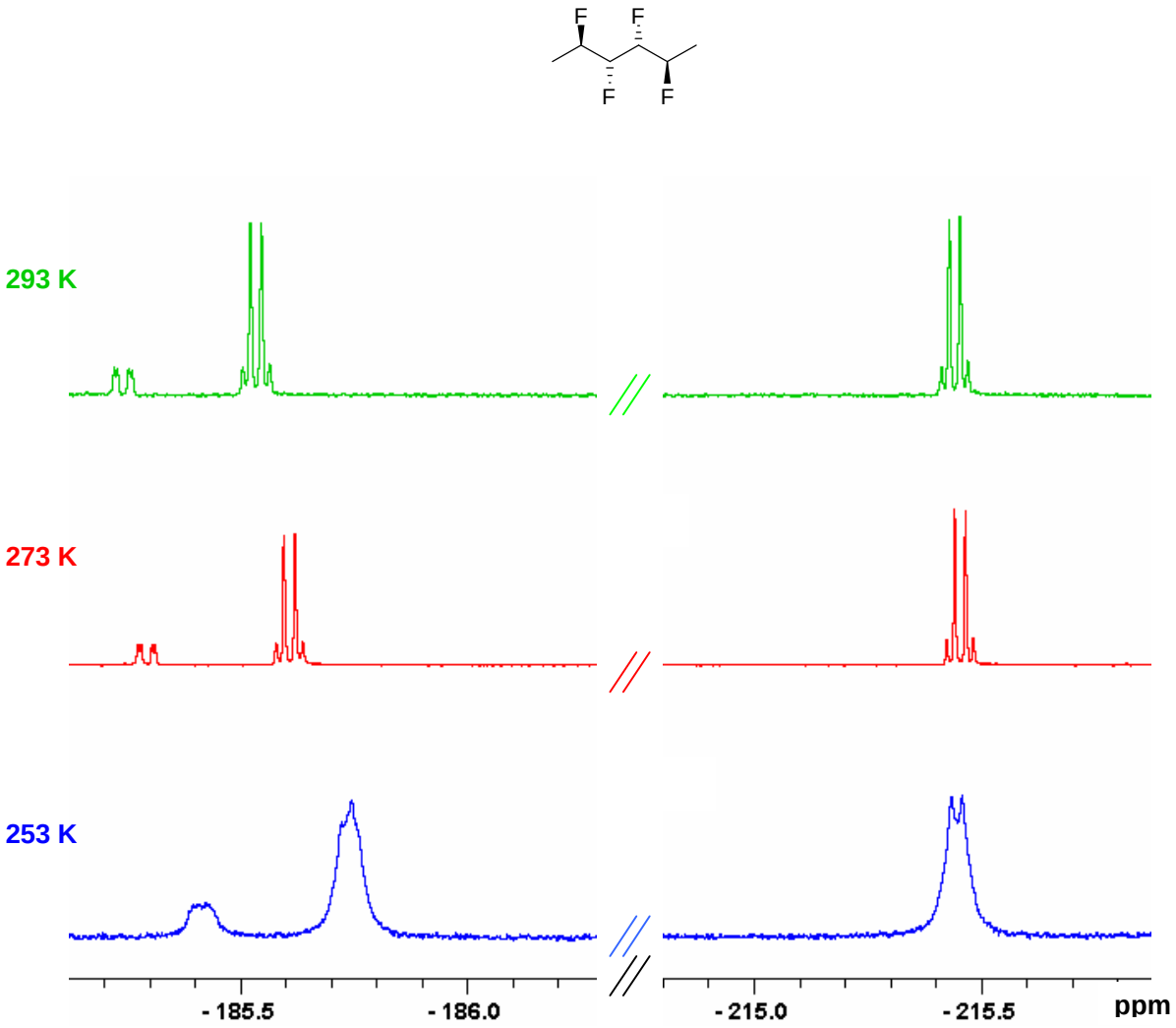

Figure S16. ^{1}H NMR (400 MHz, 81:19 v/v $CDCl_3/D_8$-THF) of **1c**

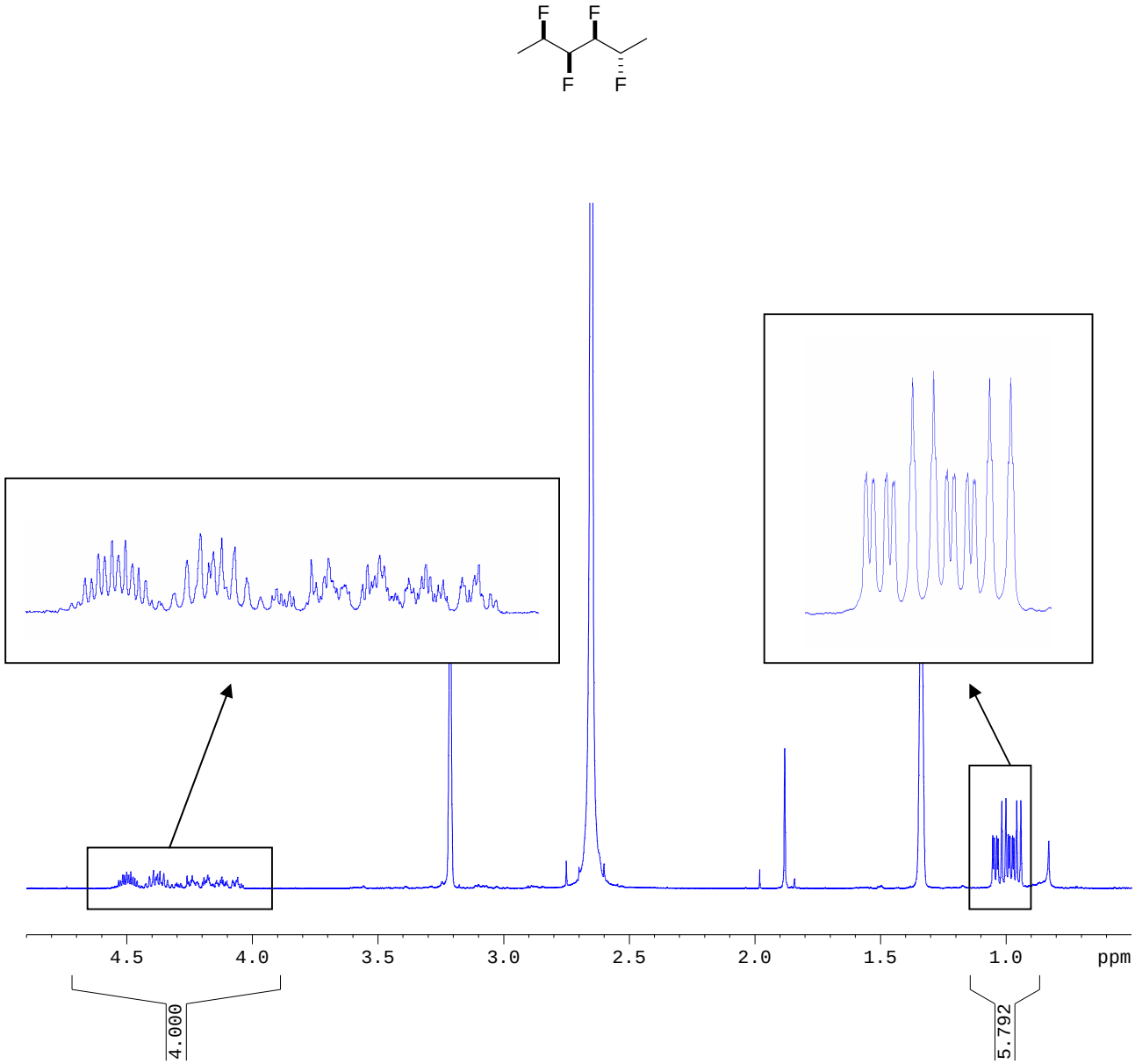

Figure S17. $^{1}H,^{1}H$ 2D-COSY NMR (400 MHz, 81:19 v/v $CDCl_3/D_8$-THF) of **1c**

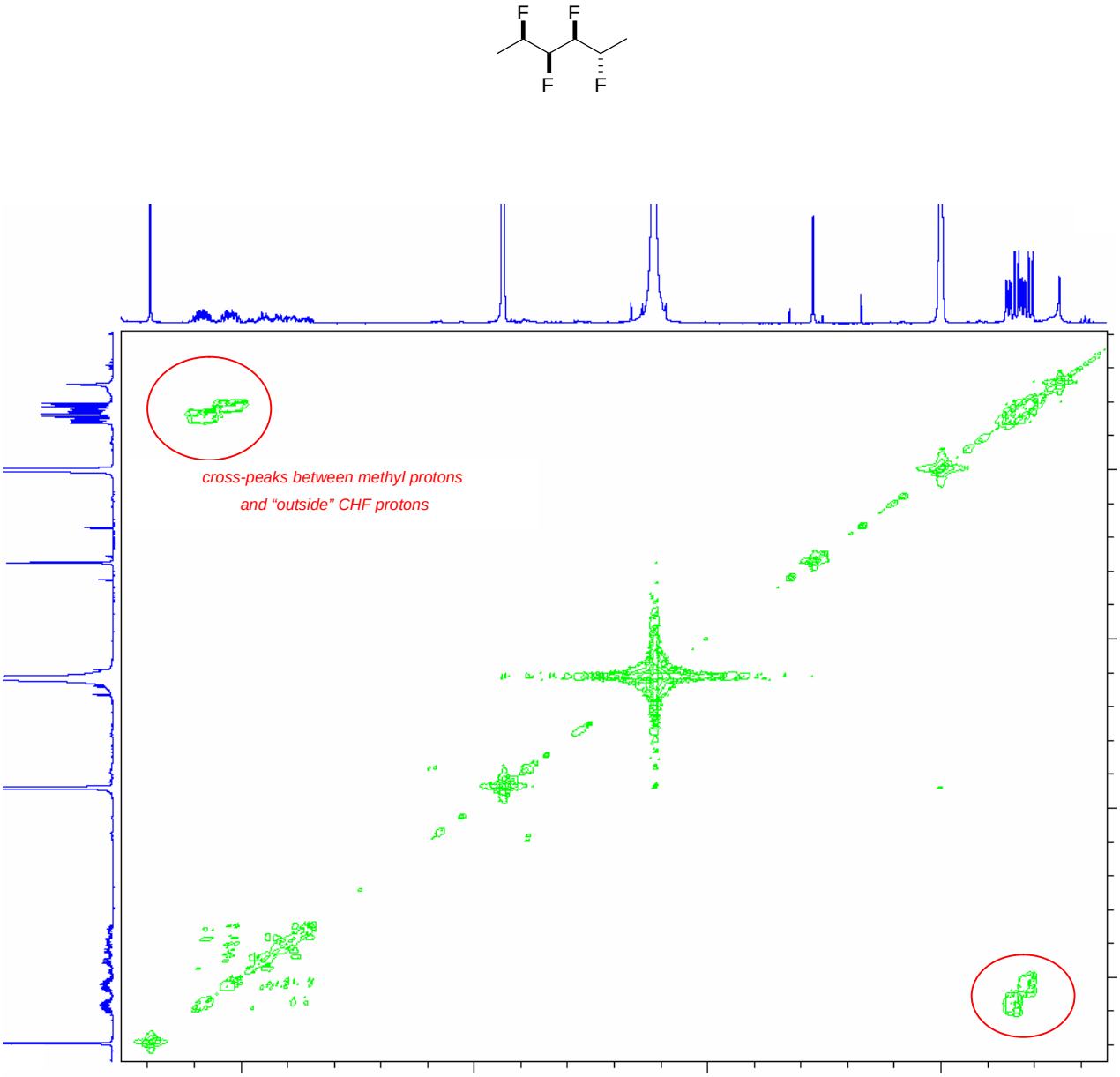

Figure S18. ^{19}F NMR (376 MHz, 81:19 v/v $CDCl_3/D_8$-THF) of **1c**

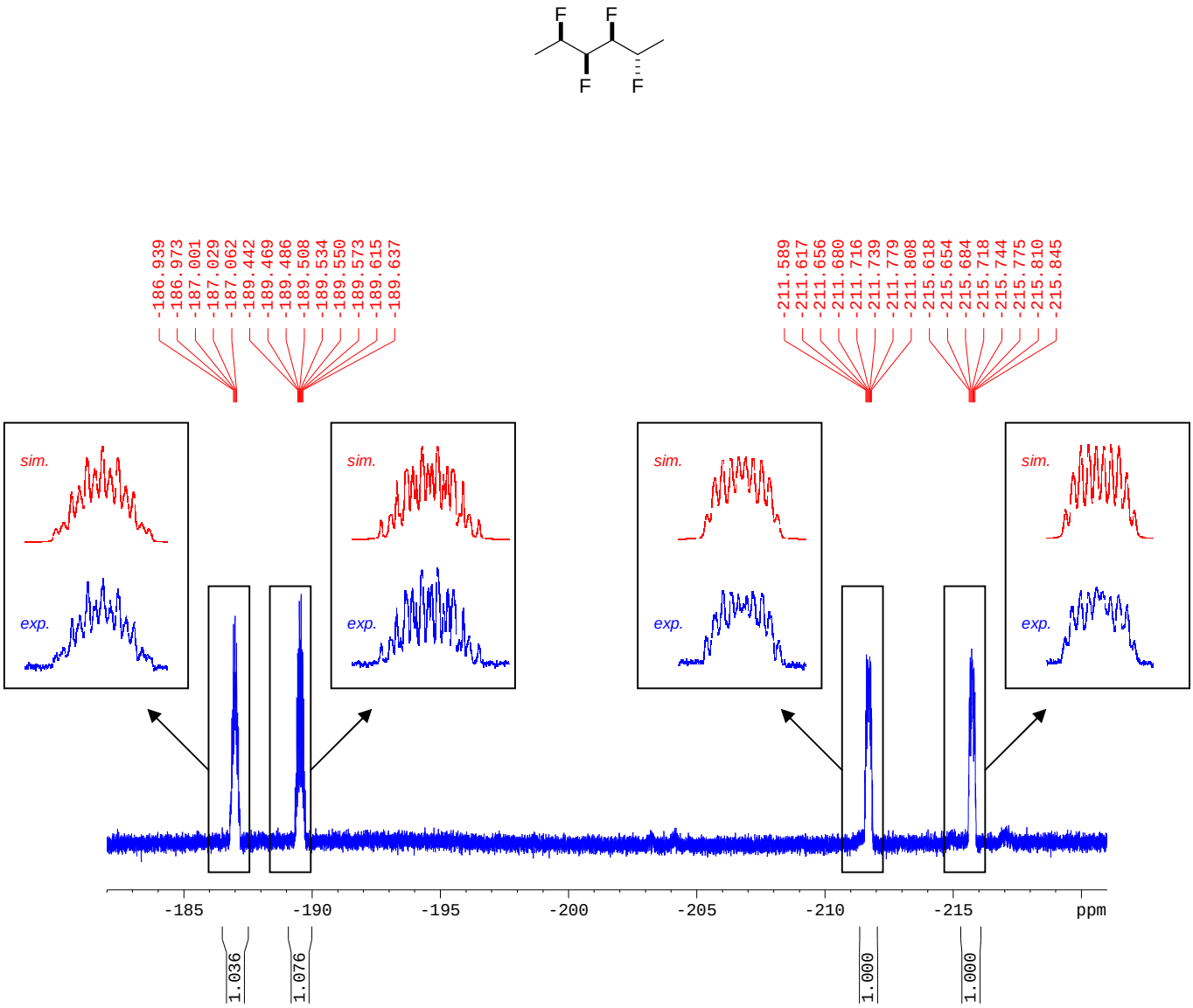

Figure S19.[a] ^{19}F {^{1}H dec} NMR (376 MHz, 81:19 v/v $CDCl_3/D_8$-THF) of **1c**

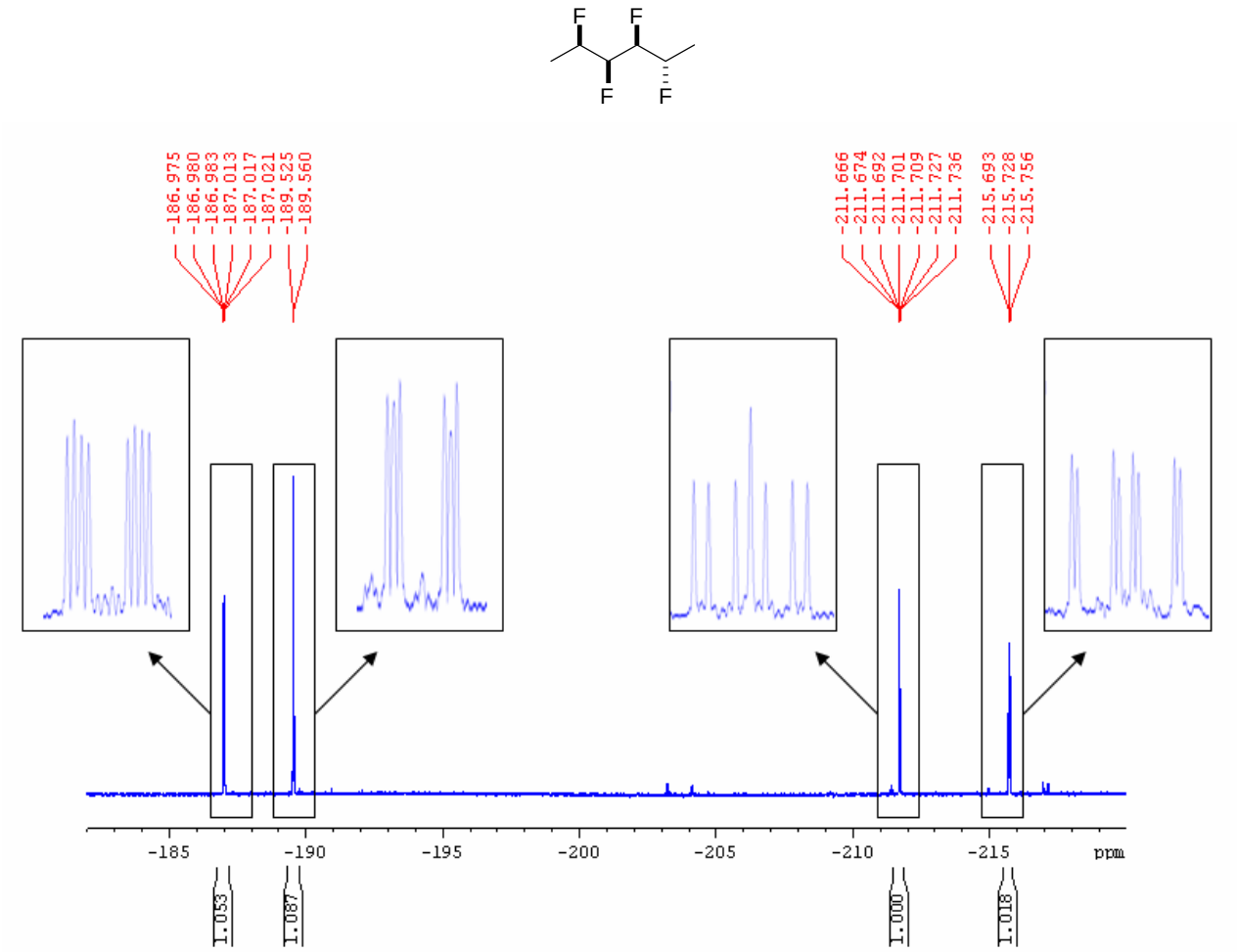

[a] The expansions are projections from the ^{19}F homonuclear *J*-resolved spectrum with ^{1}H decoupling.

Figure S20. 2D $^{1}H,^{13}C$ HSQC with adiabatic pulses (500 MHz, 81:19 v/v $CDCl_3/D_8$-THF) of **1c**

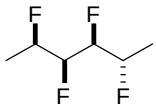

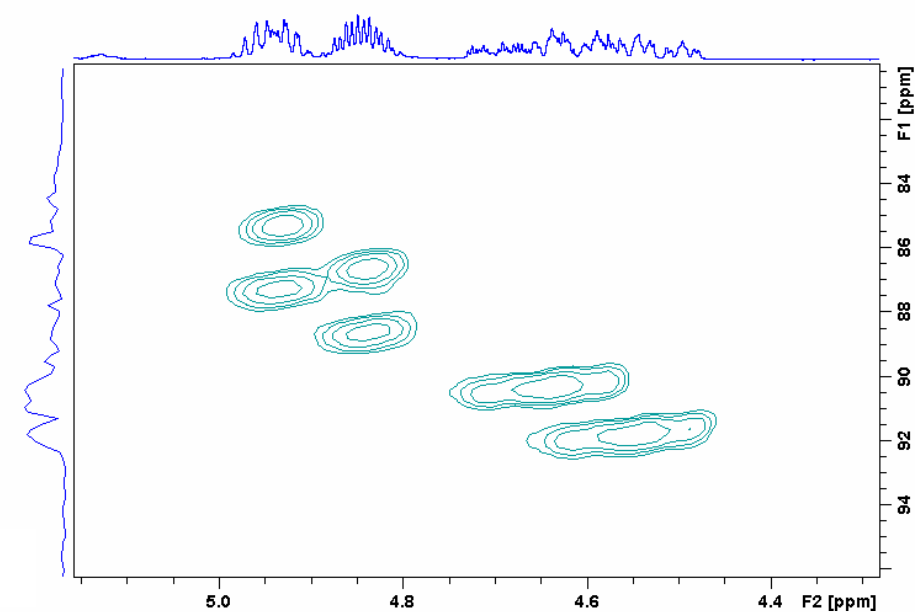

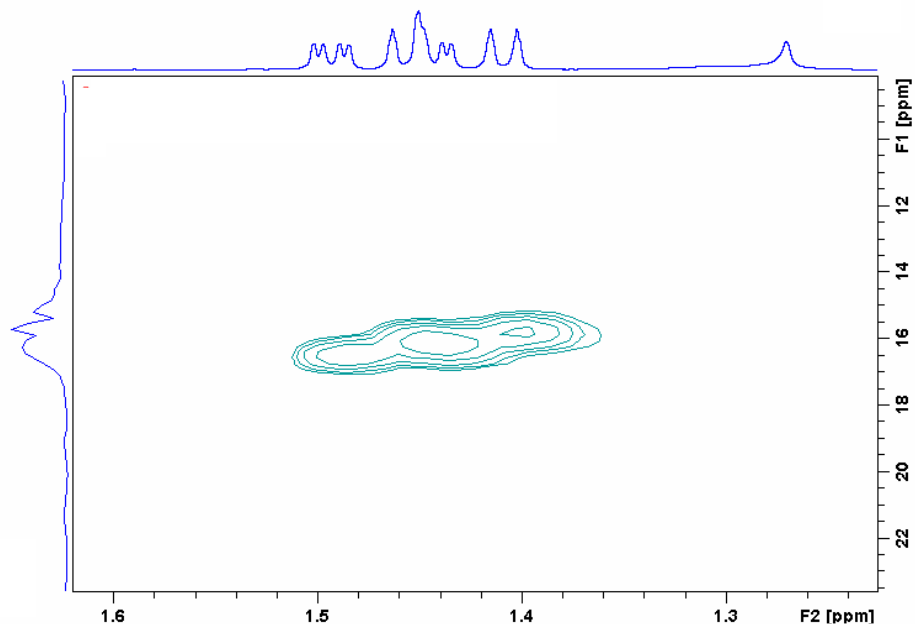

Table S3.[a] Calculated coupling constants for **1c**

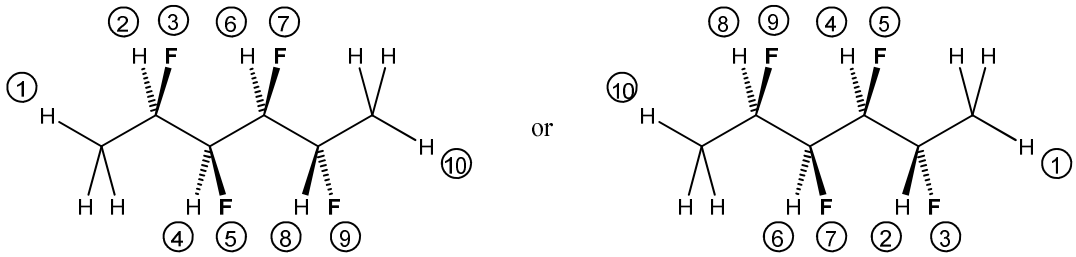

	2	**3**	**4**	**5**	**6**	**7**	**8**	**9**	**10**
1	6.5	24.5	0.0	2.0	0.0	0.5	0.0	0.0	0.0
2		47.0	6.4	12.0	0.0	0.0	0.0	0.0	0.0
3			9.1	14.2	2.0	3.4	0.0	1.6	0.0
4				47.0	2.5	26.0	0.0	0.6	0.0
5					24.0	9.8	0.0	1.4	0.5
6						47.0	6.0	16.7	0.0
7							13.0	13.2	2.0
8								47.0	6.5
9									24.5

[a] Coupling constants were determined by a five-step process:

1. Inspection of the ^{19}F {^{1}H dec} NMR spectrum (Figure S19) provided all $^{3}J_{FF}$, $^{4}J_{FF}$ and $^{5}J_{FF}$ values, which allowed all fluorine signals (**3**, **5**, **7** and **9**) to be assigned;
2. The ^{19}F NMR spectrum (Figure S18) was then simulated, giving all $^{3}J_{HF}$ values;
3. Inspection of the ^{1}H,^{1}H 2D-COSY NMR spectrum (Figure S17) allowed signals corresponding to the "outside CHF protons" (**2** and **8**, $\delta \sim 4.4$ ppm) to be distinguished from the "inside CHF protons" (**4** and **6**, $\delta \sim 4.1$ ppm);
4. Inspection of the "inside CHF protons" region of the ^{1}H NMR spectrum (Figure S16) revealed that one multiplet (δ 4.19 ppm) contained a coupling constant of 9.1 Hz, while the other (δ 4.24 ppm) contained a coupling constant of 16.7 Hz; these values were cross-checked against the $^{3}J_{HF}$ values from the simulated ^{19}F NMR spectrum (Figure S18), which allowed protons **4** and **6** to be unambiguously assigned to their respective signals;
5. Further inspection of the multiplets corresponding to protons **4** and **6** in the ^{1}H NMR spectrum (Figure S16) revealed the $^{3}J_{HH}$ values between protons (**2** and **4**), (**4** and **6**), and (**6** and **8**).

This five-step process provided a complete "map" of $^{3}J_{HF}$ and $^{3}J_{HH}$ values. It should be emphasised that there remains an ambiguity because this "map" of *J* values suggests a symmetrical pattern of *gauche* and *anti* H-C-C-F and H-C-C-H angles, and the "map" of *J* values could fit the molecule in either of two orientations (see structures above). Nevertheless, both orientations of the "map" of *J* values suggest the same molecular conformation.

Figure S21. Variable-temperature ^{1}H NMR (500 MHz, 81:19 v/v $CDCl_3/D_8$-THF) of **1c**

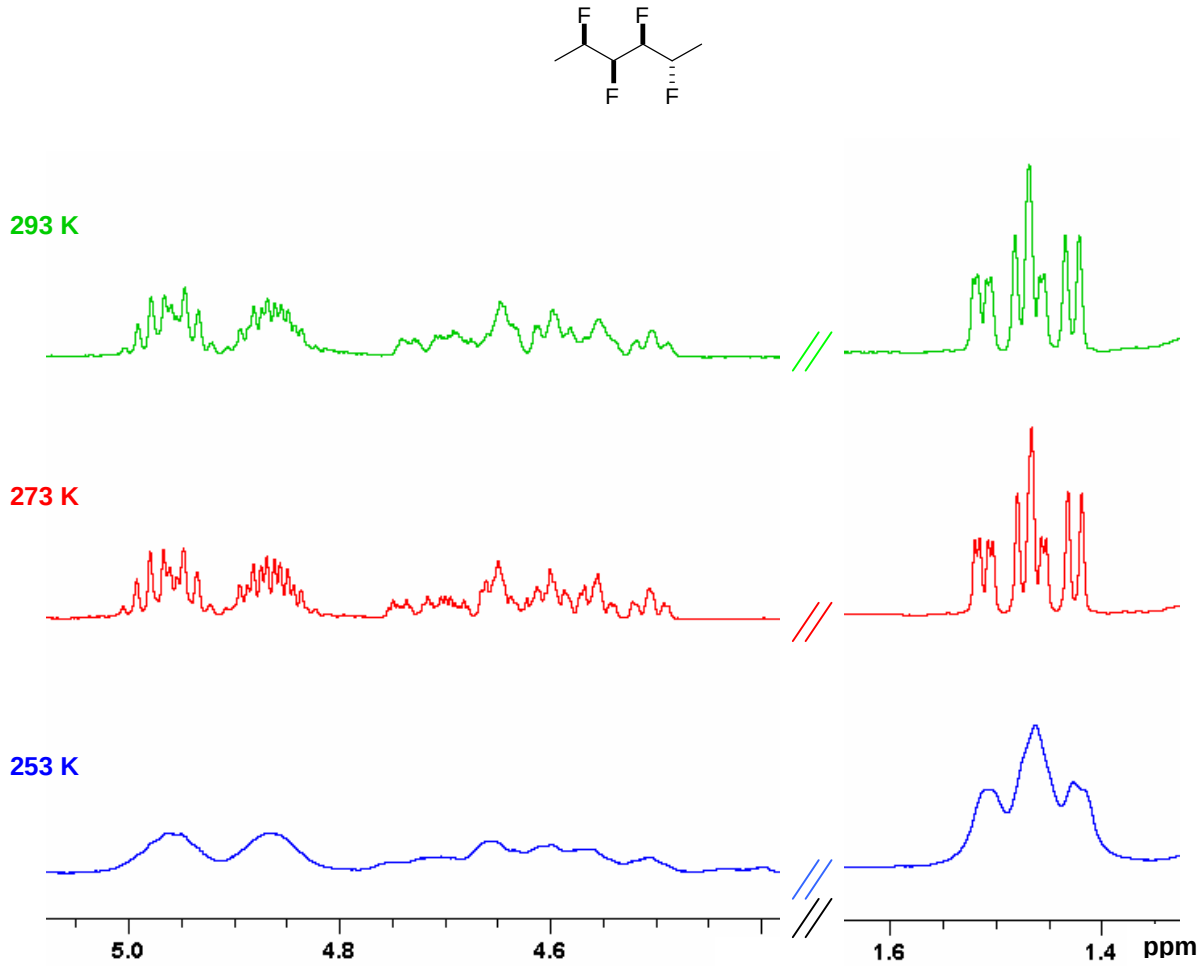

Figure S22. Variable-temperature ^{19}F NMR (470 MHz, 81:19 v/v $CDCl_3$/D_8-THF) of **1c**

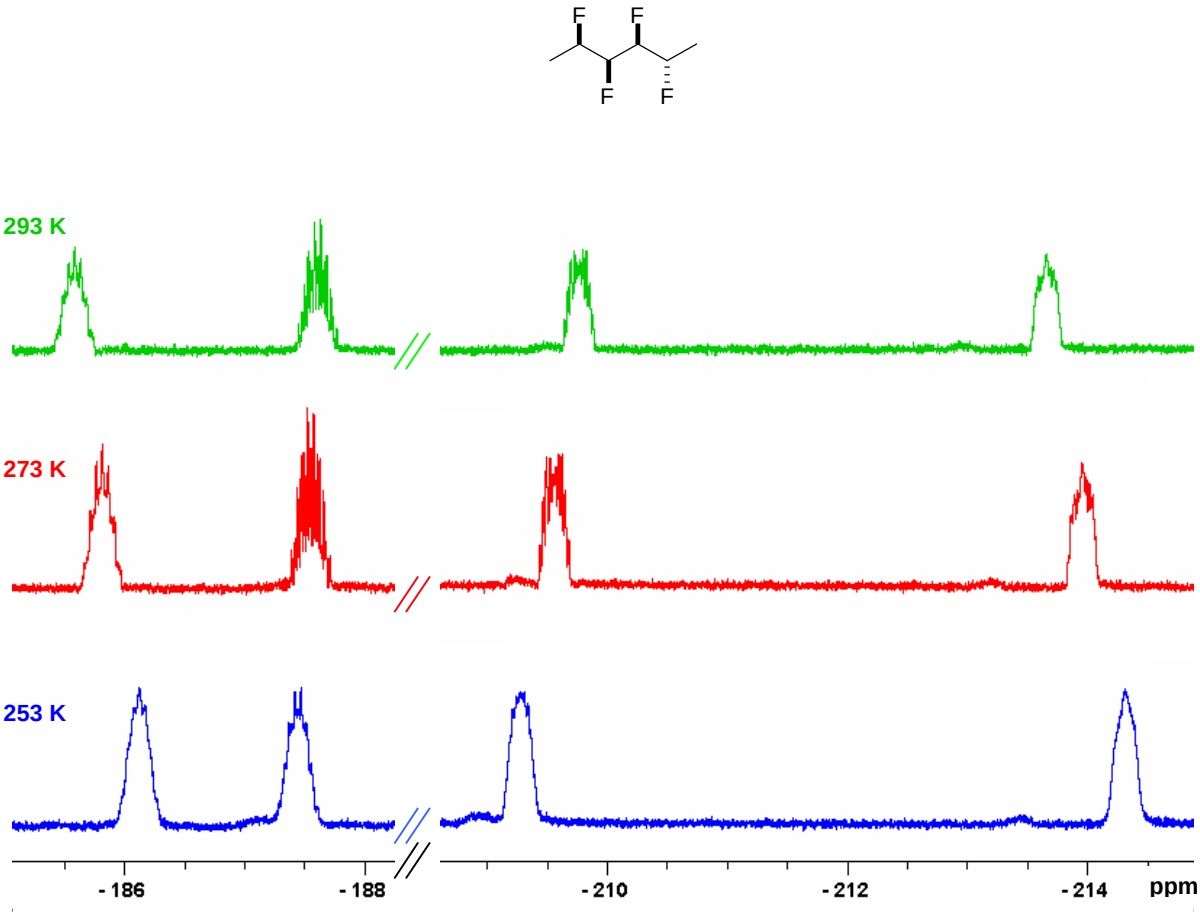

Figure S23. Variable-temperature ^{19}F {^{1}H dec} NMR (470 MHz, 81:19 v/v $CDCl_3/D_8$-THF) of **1c**

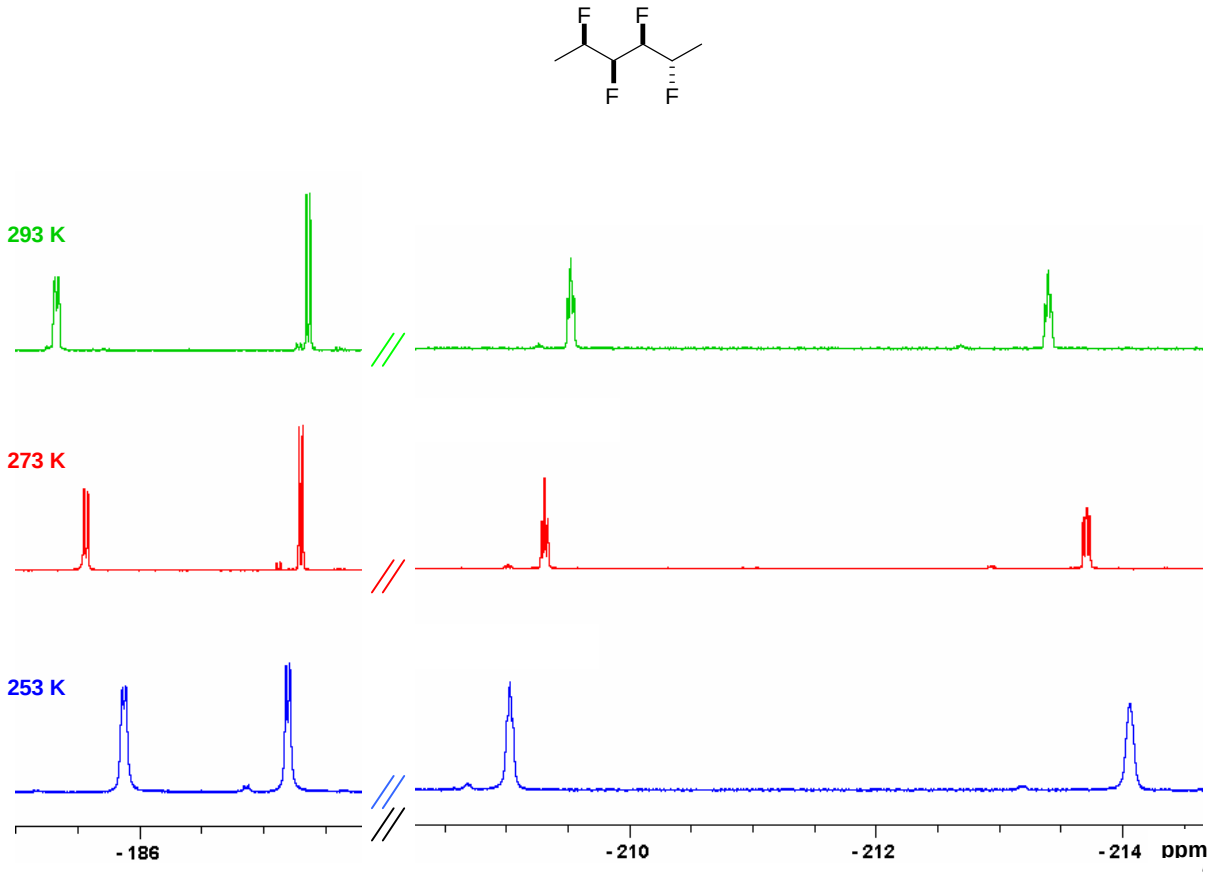

Figure S24. GC-MS (CI, +ve) spectrum of **1a**:

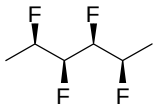

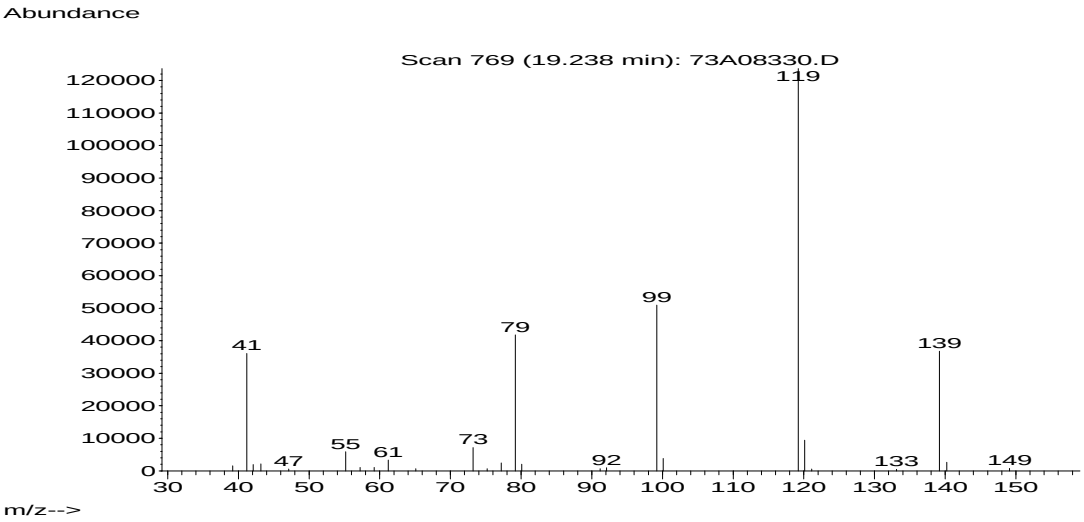

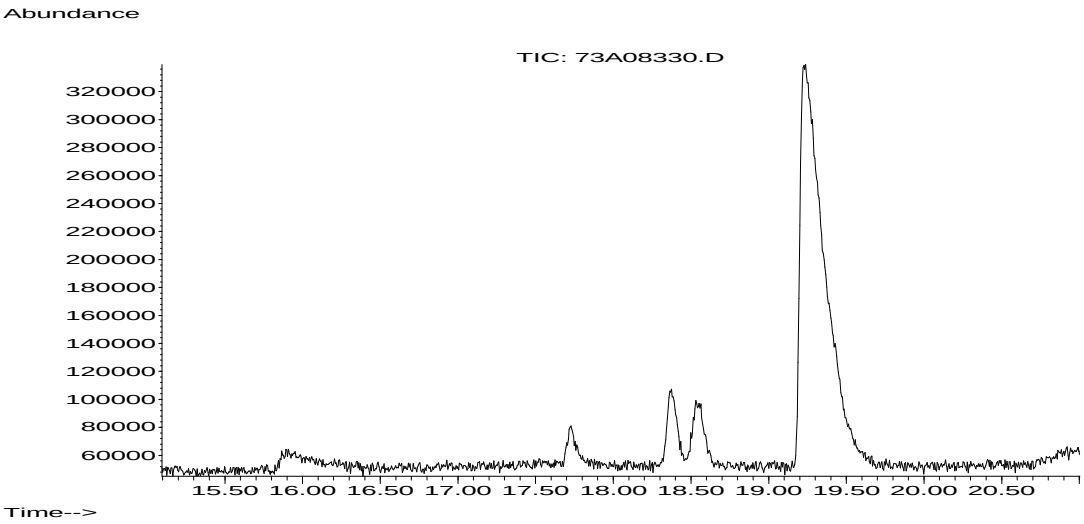

Figure S25. GC-MS (CI, +ve) spectrum of **1b**:

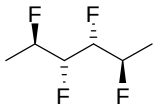

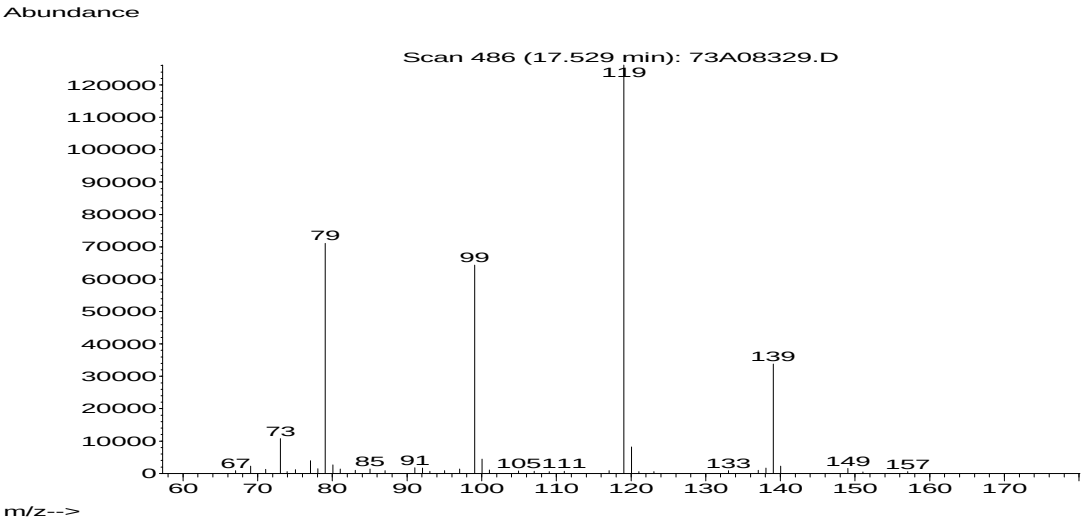

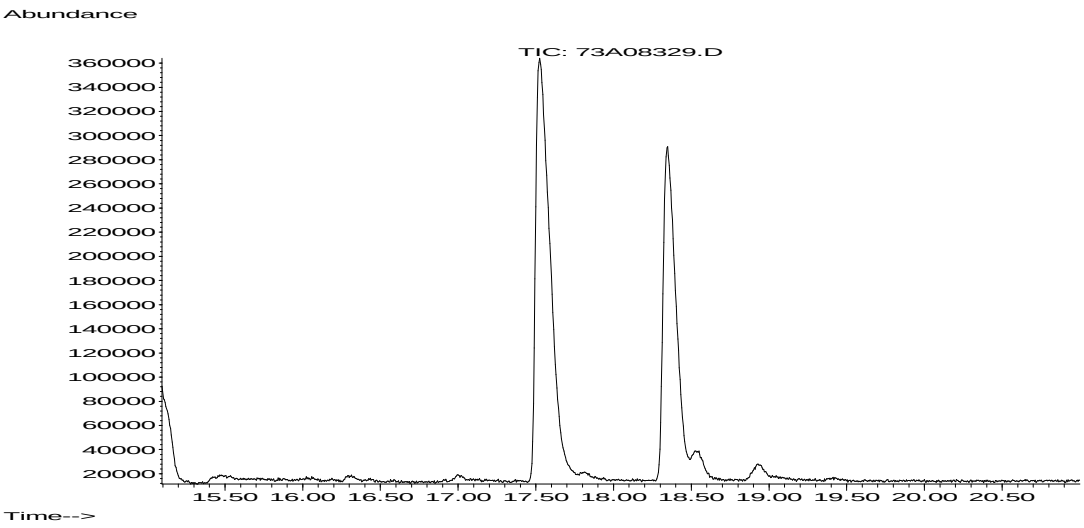

Figure S26. GC-MS (CI, +ve) spectrum of **1c**

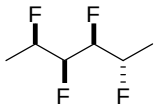

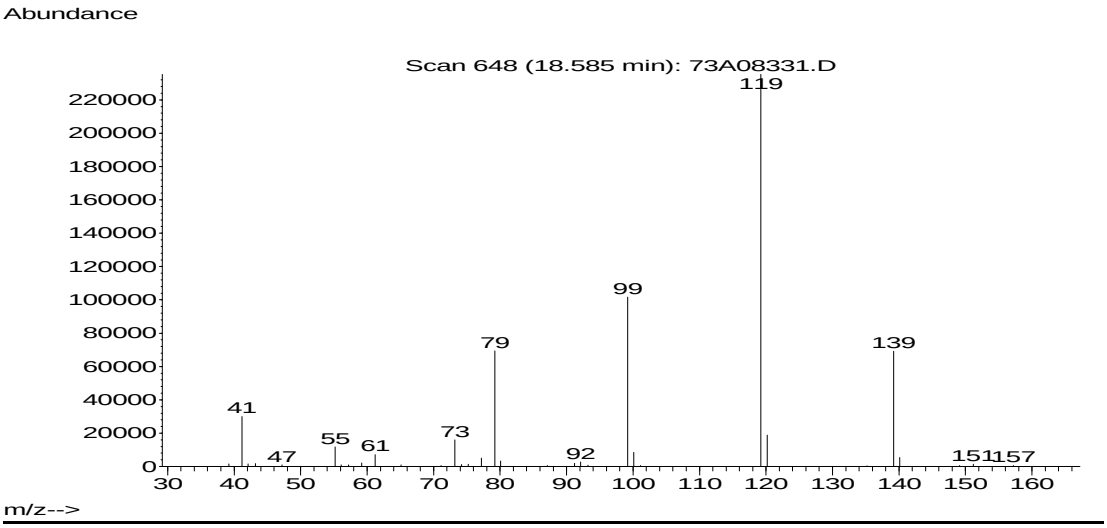

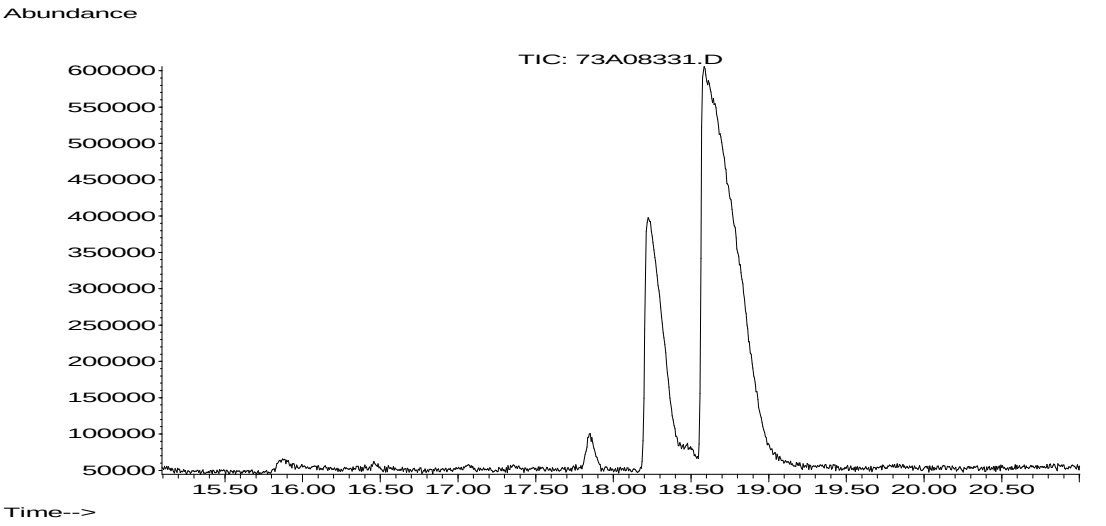

Table S4. Computational details for minimum-energy conformers of **1a–c**.

Compound	**1a**	**1b**	**1c**
Minimum-energy conformation[1]	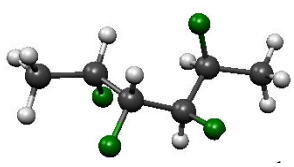	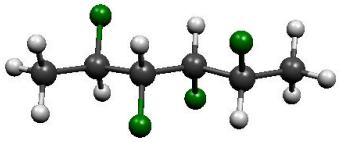	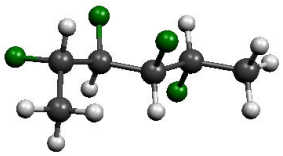
Geometry	B3LYP/6–31G(d)	B3LYP/6–31G(d)	B3LYP/6–31G(d)
E (a.u.)	–634.01335330	–634.01433900	–634.01169980
E (kcal/mol)	–397843.37919575	–397843.99772250	–397842.34162450
ZPE (kcal/mol)	100.30415000	100.00460000	100.17691000
E + ZPE (kcal/mol)	–397743.07504575	–397743.99312250	–397742.16471450
Single point	B3LYP/6–311+G(2d,p)	B3LYP/6–311+G(2d,p)	B3LYP/6–311+G(2d,p)
E (a.u.)	–634.24446510	–634.24575530	–634.24347620
E (kcal/mol)	–397988.40185025	–397989.21145075	–397987.78131550
E + ZPE (kcal/mol)	–397888.09770025	–397889.20685075	–397887.60440550
ΔE (kcal/mol)	**–5.86**	**0.00**	**–1.66**
Single point	MP2/6–311+G(2d,p)	MP2/6–311+G(2d,p)	MP2/6–311+G(2d,p)
E (a.u.)	–632.81184240	–632.81202890	–632.81039440
E (kcal/mol)	–397089.43110600	–397089.54813475	–397088.52248600
E + ZPE (kcal/mol)	–396989.12695600	–396989.54353475	–396988.34557600
ΔE (kcal/mol)	**–6.50**	**0.00**	**–2.16**
Dipole (D)	**2.19**	**0.25**	**3.54**
Surface area (Å^2)	**187.406**	**190.691**	**190.285**
Volume (Å^3)	**165.497**	**166.306**	**166.226**

Figure S27. Molecular dipole moment for alternative conformer of **1c** [B3LYP/6–311+G(d,p)]

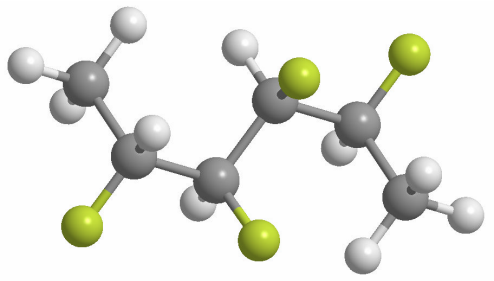

Dipole = 1.4199 D